3-D Ray-Tracing Simulations for 5.7GHz RF Indoor Position Location System

Venu Annamraju and Thomas Burns
Kurt Kosbar Faculty Advisor
Department of Electrical & Computer Engineering
University of Missouri-Rolla
Rolla, MO 65409-0400

ABSTRACT

The objective of the project is to continuously track a handheld device in an office, with centimeter accuracy in the three dimensions. A 3-D ray-tracing algorithm has been developed to simulate the impulse response of the indoor channel. The algorithm can evaluate the impulse response at multiple receiver locations. Non-linear optimization has been used to eliminate the need for multiple runs of simulation. The optimization program also significantly reduces the number of rays launched. The algorithm incorporates bandwidth effects on multipath resolution of the system.

KEY WORDS

RF methods, 3-D, Ray-tracing, Position Location, Indoor Channel, 5.7GHz, ISM.

INTRODUCTION

This paper addresses key issues of a "modified brute-force" 3-D Ray-tracing algorithm that can simulate the indoor environment. Ray tracing has been a useful tool for predicting impulse response and power-delay profile of an indoor channel for LAN and mobile radio applications. Modeling the RF indoor channel provides useful insight to the problem of indoor position location. Knowledge of the channel model enables design of a suitable architecture for indoor geolocation. Intuitively, the 3-D method provides a better channel model than its 2-D counterpart. This is because in an office or factory setting, the height of the structure is comparable with the other two dimensions and thus cannot be neglected.

The paper discusses the implementation and performance of the 3-D ray-tracing algorithm. The algorithm can evaluate the impulse response at multiple receiver locations. Conventionally, obtaining receiver responses for a moving transmitter requires multiple runs of simulation. Non-linear optimization has been employed to reduce the computation time of such a task. The optimization program also significantly reduces the number of rays launched. The algorithm incorporates bandwidth effects on multipath resolution of the system. Data from simulation is used in a position estimation algorithm that simulates the overall performance of the system.

3-D RAY-TRACING

Ray-tracing techniques were first developed for use in computer graphics. These algorithms recreated an image scene under different lighting conditions and enhanced visual perception. 2-D ray-tracing algorithms have been used extensively for cellular and LAN site planning [1]. Such algorithms mainly predicted delay-spread of the impulse response and attenuation of the signal. Also since the third dimension is small comparable to the other dimensions, the 2-D method is reasonable to use in most cases. The same algorithm cannot be applied to indoor position location, because the height dimension is significant compared to length and breadth. To improve upon the accuracy in channel response predictions, 3-D modeling is required [2].

The Line-of-Sight (LOS) component of the received signal plays a dominant role in position location algorithms. Isolating the LOS signal is critical in obtaining an accurate estimate. In the outdoor environment, scatterers are located far enough apart that often each multipath component can be resolved by the virtue of system bandwidth. In the indoor environment the multipath can be so severe that the system bandwidth would not suffice in isolating the LOS from multipath components. In such a situation, other methods of position estimation need to be investigated.

MATHEMATICAL DESCRIPTION

The ray-tracing algorithm is based on the assumption that high frequency electromagnetic radiation has ray-like properties and its propagation in space can hence be modeled as a vector with power and phase. The power of the ray is attenuated by a path-dependant loss, reflections and transmissions. The phase of the ray is affected by reflections and transmissions because of the complex nature of the reflection coefficient and permittivity of the surface the ray impinges on [8]. The phase is also determined by the response of the indoor channel. The ray is also affected by diffraction but is not necessarily modeled for the indoor channel. Effects of diffraction are more significant in urban environment.

The algorithm can be implemented in any of 3 coordinate systems, namely, Cartesian, Spherical or Cylindrical coordinates. The 2-D simulation was done using polar coordinates in earlier work [3]. For simulation in 3-D, Spherical coordinate system was initially chosen as a natural extension to the polar form. However, representation of planes and lines and computing their intersections proved to be an unnecessary expense in computation time. The Cartesian coordinate was eventually chosen and the objects in the simulation were represented in the parametric form. The parametric form had the advantage that the intersection between a line and plane can be efficiently solved through matrix manipulations.

The algorithm begins with launching rays in all directions, each ray representing a wavefront. The intersections of rays with the objects in the room are computed. A corresponding angle of reflectance is calculated and the ray is checked for transmission through the surface. The power after each reflection/transmission and cumulative path length are stored as an attribute of the ray. The process is repeated until each ray is terminated based upon a set of conditions. Subsequently, each segment of a ray is checked for intersection with the receiver. For a valid intersection, the power and the path length characterize a multipath component.

RAY LAUNCHING

There are many ray launching techniques [4]. All these methods have the equidistant constraint on angular spacing. The minimum angular separation determines the total number of rays that is launched. The total number of rays launched is approximately given by

$$\text{Number of rays launched} = (2\pi/\alpha)[(\pi/\alpha) -1] +2$$

where α is the angular spacing in radians. The number of rays increases with the angular spacing squared. An angular separation of 5 degrees created approximately 2500 rays from the source. Figure 1 shows that the rays are more closely spaced near the poles than at the equator. At the outset the ray launch algorithm seems to be in violation of the usual constraint on angular spacing, but it does not introduce any error in calculations. The effect is an increase in the ray launching time by approximately 12% causing a similar increase in the simulation time. The exact increase in time is dependant on the placement of transmitter and receivers and the channel structure. The net increase in simulation time is reduced when computing response for 20 or more transmitter positions using the optimization routine.

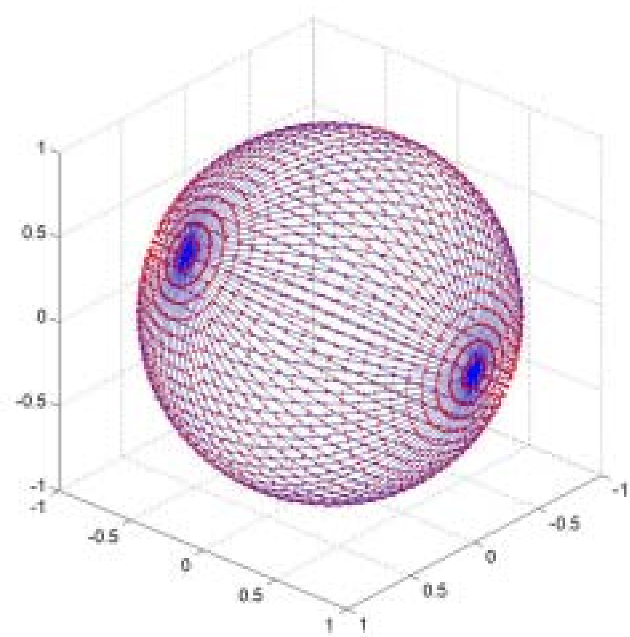

Figure 1. Ray Launching Angles

The choice of angular spacing also bounds the dimension of an object that can be modeled. This holds significance especially when low order reflections are considered. Adjacent rays can miss a valid reflection off a small object due to large angular spacing. Previous work has established that effect of small objects on the overall channel response is insignificant [5].

RAY-WALL INTERSECTION

The vertex coordinates for a wall are specified in Cartesian coordinates in a file. The order of vertices and the attenuation characteristics for each wall is specified in another file. The vertex coordinates are used to frame equations representing each wall. The intersection of each ray and a wall is accomplished through efficient matrix computation. A ray is terminated when it exceeds a specified number of reflections. The default case of termination occurs when the power level falls below the threshold of the receiver. The relative permittivity, ε_r and conductance, σ of a building material is used to calculate the power loss of a ray due to reflections and transmission. The power level is also dependent on the angle of incidence of the ray. In practice, these values are not constant for a material. The material is also heterogeneous in composition, and so a range of values binds the above parameters [6].

The uncertainty has been avoided by exploring other ways to characterize building materials for ray tracing. One approach is to associate a scalar Reflection Coefficient to a material that remains insensitive to angle of incidence [6]. The value chosen is one that best fits an elaborate measurement data. Another way is to set the power loss due to reflection as 6dB and that due to transmission as 12dB [ref]. The above approximations have been used in many ray-tracing models to predict mainly the path loss and delay spread of the channel. The simulation uses a constant power loss for reflections and transmissions. About 6-7 reflections/transmissions are considered for the simulation.

The instantaneous carrier phase is affected by path length, random phase changes in channel and due to reflection/transmission mechanisms. The channel structure is relatively constant for transmitter motion within a few wavelengths [7]. The path length is a dominant factor that affects the phase changes of the carrier. Resolving path differences of 1cm can theoretically give us about 75 degrees phase accuracy with a small random error.

RECEIVER MODELING

Many ray-tracing models have used reception spheres to model receivers rather than a point. This is because of the finite angular separation between each ray. The radius of reception sphere is chosen carefully to avoid double counting of rays [3]. The sphere grows with increase in path length and angular spacing. The calculation error inherent to the receiver model also increases. Another type of modeling involves weighing functions for calculating the effect of each ray at the receiver. These models can be easily applied for path-loss measurements and do not effectively address the problem of position location. To accurately predict carrier phase changes occurring due to path length, smaller reception spheres are required, which increases the number of rays, which need to be launched, driving up simulation time. This makes the existing ray-tracing models inefficient, due to unreasonably high computation time.

The problem has been overcome by using two spheres of reception with different radii. The initial radius is greater than the final radius by many orders of magnitude. Keeping the angular spacing constant at 5 degrees, we have approximately 2500 rays. The initial sphere of reception is now proportional to the largest dimension of the environment. The intersection of the sphere with each segment of a ray is checked and attributes of those rays are stored. These rays are subjected to a non-linear optimization algorithm with the azimuth, θ and elevation, φ as input parameters. The angles are simultaneously varied to converge each stored ray into the smaller sphere of reception.

NON-LINEAR OPTIMIZATION

The optimization algorithm is a variation of steepest-descent method in two dimensions. A ray may achieve the performance goal if there exists a continuous path between the initial guess (θ_{ini}, φ_{ini}) and the global minimum (θ_{opt}, φ_{opt}) on the error-performance curve. In the physical sense it implies that the ray can converge to the smaller sphere of reception by reflection/transmission through a given set of objects. A ray may not converge if no such path exists, in other terms it cannot touch the new sphere by bouncing off the same objects as the initial guess. The flowchart description is shown in Figure 2. The algorithm can be broadly divided into two sections as coarse convergence and fine convergence. During coarse convergence, the algorithm moves from the initial guess towards (θ_{opt}, φ_{opt}) with a constant search radius in the direction of steepest gradient. Fine convergence begins when (θ_{opt}, φ_{opt}) is in the neighborhood of (θ_c, φ_c). The neighborhood of (θ_c, φ_c) is the set of points within a radius, σ_i.

The algorithm can converge from any direction and the resulting phase error is less than 1 degree for a Tx-Rx separation greater that 2 wavelengths. This is acceptable since centimeter accuracy in position requires a phase resolution of 72 degrees. The total number of iterations is limited to 30 by default. The time for each ray convergence depends on functional evaluations per iteration and number of iterations required for achieving the performance goal. The number of iterations depends on the initial search radius, the contraction factor and the desired goal. The algorithm is very flexible as we have choice of optimizing for speed or accuracy.

The simulation is based on the assumption that change in path length has a dominant effect on the phase change in the carrier. Simulation of transmitter motion is necessary to understand the carrier phase. A direct approach is to move the transmitter by a distance less than a wavelength and reapply the ray-tracing algorithm. This approach is computationally expensive and does not exploit the consistency of channel structure over a few wavelengths [2]. A better approach is to use the data of the previous position in the optimization algorithm described above. The algorithm assumes that the same rays will converge at the receivers for the new TX position. This assumption is however valid only for small changes in TX position. The error between the direct method and this approach is found to be less than 1 percent over movements lesser than 5 wavelengths.

TRANSMITTER MOTION

The simulation is based on the assumption that change in path length has a dominant effect on the phase change in the carrier signal. Simulation of the transmitter motion is necessary to understand the carrier phase. A direct approach is to move the transmitter by a distance less than a wavelength and reapply the ray-tracing algorithm. This approach is computationally expensive and does not exploit the consistency of channel structure over a few wavelengths. A better approach is to use the data of the previous position in the optimization algorithm described above. The algorithm assumes that the same rays will converge at the receivers for the new TX position. This assumption is however valid for small changes in TX position. The error between the direct method and this approach is found to be less than 1 percent over movements less than 5 wavelengths.

Figure 2. Non- Linear Optimization Algorithm for Ray-Tracing

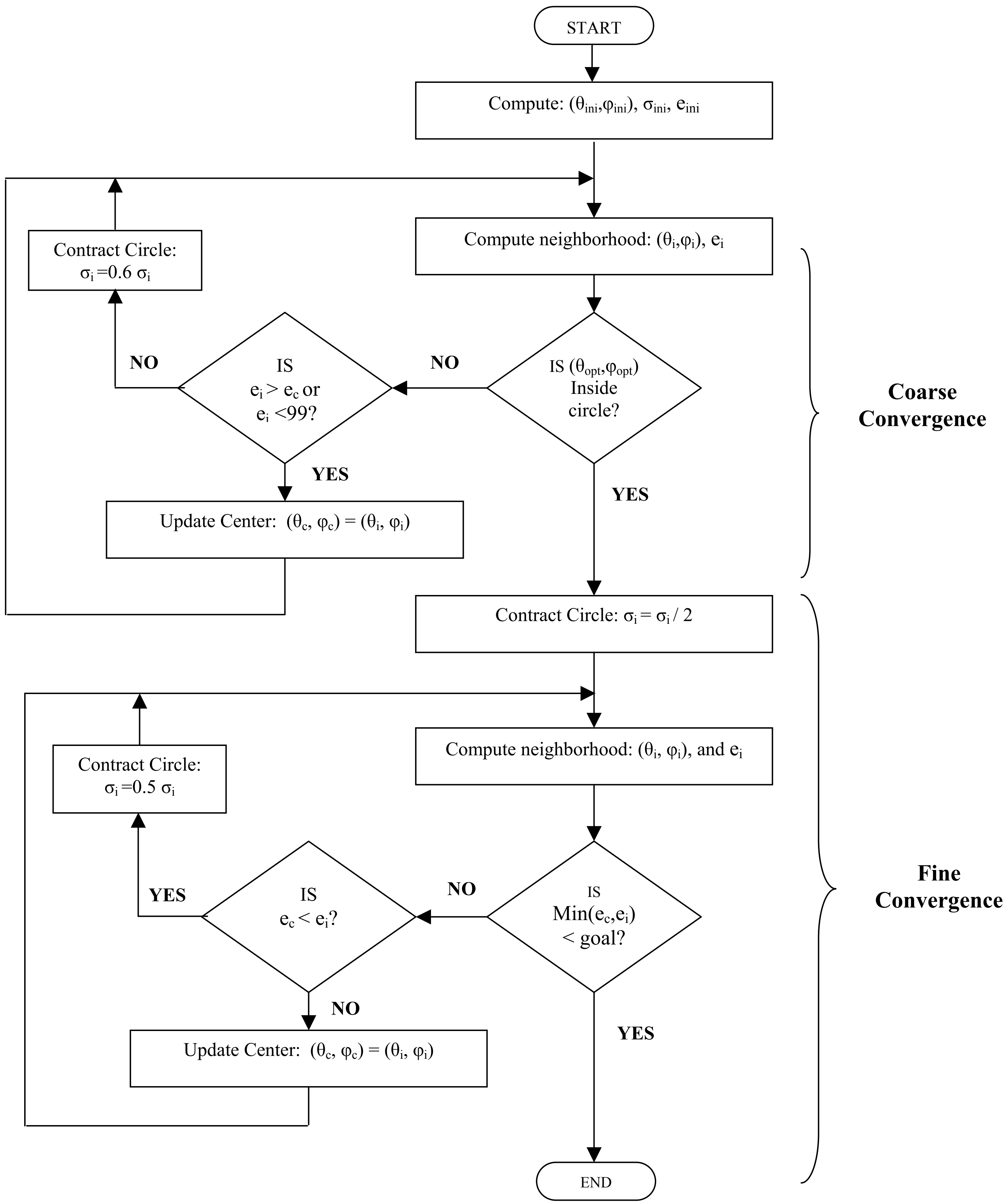

MULTIPATH RESOLUTION

The system bandwidth directly determines the multipath resolution of the received signal. The ISM band has 200MHz available bandwidth that corresponds to 5ns resolution. Developing systems to work with 200MHz bandwidth is expensive and tends to defeat the purpose. It is observed from HiperLAN measurements at 5.8GHz that multipath in indoor environments fades out within 200ns [9]. From the simulation it is seen that the spacing between multipath components can be as small as 0.1ns. Thus it is evident that aiming for higher bandwidth does not come across as feasible solution. The phase of LOS ray is thus corrupted by the adjacent multipath components. The relative power of multipath and the LOS is indicative of the extent to which the phase is corrupted. Phase corruption is more in an environment with metal furniture and cabinets, since a metallic surface acts as a good reflector. Attempting to accurately determine the phase of LOS ray may not be possible.

RESULTS AND CONCLUSION

The ray tracing software is provided with a user interface that has debug options to verify stages of the simulation process. Debugging options include viewing a 3-D room setup, TX and RX locations, launched rays, rays intersecting initial sphere of reception, rays with unique paths, optimization process for each ray, converged rays for each receiver, phase, amplitude response for each receiver and response of bandwidth-limited system.

The program retains options from the previous simulation run. Parameters such as TX carrier frequency, TX power, RX sensitivity, PN chip frequency, chip length and maximum number of bounces. The interface was helpful during initial testing and verification of the ray tracing software.

A variety of programs have been developed for data measurement and analysis. A testing program generates phase and amplitude errors occurring in TX motion simulation. The phase error between the direct method and optimization approach is determined by the program. A plotting program generates surfaces representing carrier phase changes due to transmitter motion. This helps in understanding phase variation in the channel. A software driver has been developed for the algorithm that generates a large database by varying parameters such as number of reflections, receivers, TX-RX separation. Another program is set up to measure simulation time with varying number of objects in the environment. The data is used by a plotting program to generate plots between any 2 of 10 different variables. The graphs illustrate the interdependence between the different parameters. They are used as benchmarks while modifying the algorithm for speed or accuracy.

The simulation time is determined by the maximum allowable reflections as shown in Figure 3. The simulation time has an exponential relationship with the maximum allowable reflections. The number of rays intersecting the initial sphere is far greater than the converged rays. For a particular order of reflection the average time for a ray to converge varies with the initial guess and the global minima as seen in Figure 5. A ray may be optimized anywhere within 30 iterations, hence the variation in time in Figure 5. The maximum time is bounded by the average non-convergence time. For the case of a non-convergent ray in Figure 6, the time taken remains relatively constant because every such ray iterates 30 times.

The parameter setting of the optimization algorithm is such that the number of rays that do not converge primarily influences the simulation. Figure 4 shows the percentage of time wasted in the process for varying number of reflections. Figure 7 contains typical simulation times for converging and non-converging rays. The total number of rays that need optimization is very high as compared to the number of unique paths since many of the rays have similar paths. This is not wasteful, since we optimize the same set of rays for many TX positions. Also, if all possible multipath components need be detected, it is necessary to use all the rays intersecting the initial sphere of reception. The total time can be greatly reduced if a small error can be tolerated. In such a case only unique ray paths need optimization.

If a large number of walls are present, the algorithm can be modified to optimize only for unique paths. The phase error due to the modification is shown in Figure 8. The effect of taking smaller steps tends to reduce the variance of phase error. This error occurs randomly and can be treated as noise in the measurement. For a 1cm step, the maximum error is about 6 degrees.

In the context of the present problem, 3-D ray tracing helps characterize the phase profile the indoor channel with a greater degree of accuracy compared to 2-D methods. The model bases itself on the assumption that path length between the TX and RX affects the carrier phase. Motion of the transmitter can be realized using the optimization algorithm. Simulation data is being used to develop means of position estimation that is independent of the RX positions.

REFERENCES

[1] Measuring, modeling, and characterizing of indoor radio channel at 5.8 GHz, Cuinas, I.; Sanchez, M.G., Vehicular Technology, IEEE Transactions on, Volume: 50 Issue: 2 , March 2001,Page(s): 526 – 535

[2] A three-dimensional image ray tracing (3D-IRT) method for indoor wireless channel characterization, Naruniranat, S.; Yi Huang; Parsons, D. High Frequency Postgraduate Student Colloquium, 1999 , 1999, Page(s): 62 -67

[3] Conceptual design of a centimeter accuracy local positioning system, Venu Annamraju, Kurt Kosbar International Telemetering Conference Proc., October 2001

[4] A ray tracing method for predicting path loss and delay spread in microcellular environments, K.R. Schaubach, N.J. Davis, T.S. Rappaport, IEEE Vehicular,Tech. Conference, vol. 2, 1992, pp. 932 –935.

[5] A graphical indoor radio channel simulator using 2D ray tracing, Holt, T.; Pahlavan, K.; Lee, J.F. Personal, Indoor and Mobile Radio Communications, 1992. Proceedings, PIMRC '92., Third IEEE International Symposium on , 1992,Page(s): 411 -416

[6] Wideband measurement and analysis of penetration loss in the 5 GHz band, Karlsson, P.; Bergljung, C.; Thomsen, E.; Borjeson, H. Vehicular Technology Conference, 1999. VTC 1999 - Fall. IEEE VTS 50th , Volume: 4 , 1999 Page(s): 2323 -2328 vol.4

[7] The indoor radio propagation channel, Hashemi H., Proceedings of the IEEE, Volume: 81 Issue: 7, July 1993, Page(s): 943 -968

[8] In situ microwave reflection coefficient measurements for smooth and rough exterior wall surfaces Landron, O.; Feuerstein, M.J.; Rappaport, T.S. Vehicular Technology Conference, 1993., 43rd IEEE , 1993 Page(s): 77 –80

[9] Modeling the HIPERLAN radio channel, *Halls, G.A.* Personal, Indoor and Mobile Radio Communications, 1994. Wireless Networks - Catching the Mobile Future., 5th IEEE International Symposium on , Volume: 3 , 1994 Page(s): 954 -958 vol.3

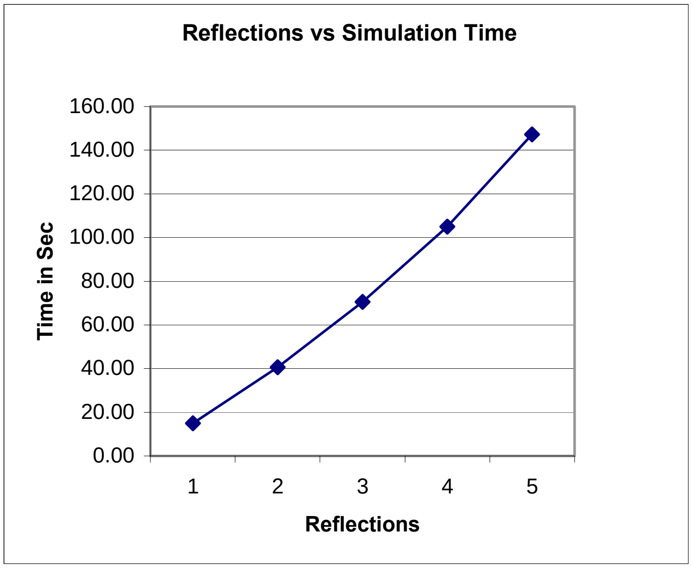

Figure 3. Plot of Simulation Time for one Receiver vs Number of Reflections averaged over 4 TX-RX distances

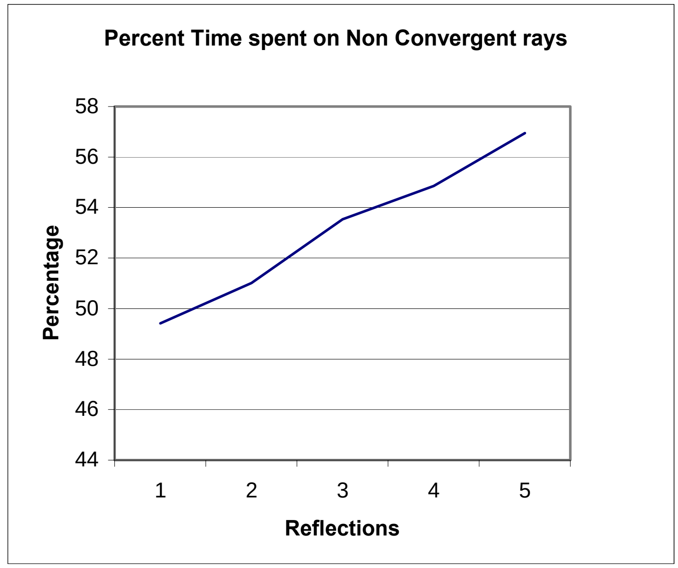

Figure 4. Plot of Percentage time spent on non-Convergent rays vs reflections averaged over 5 receivers and 4 TX-RX distances.

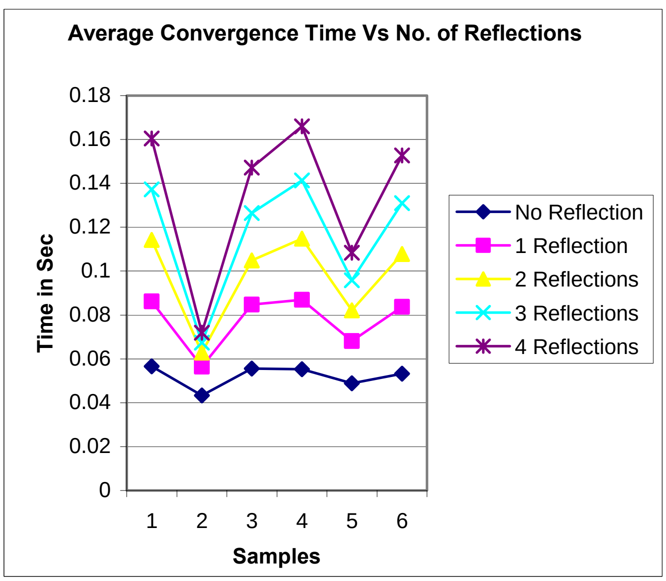

Figure 5. Plot of Average convergence time vs samples averaged over 5 Receivers

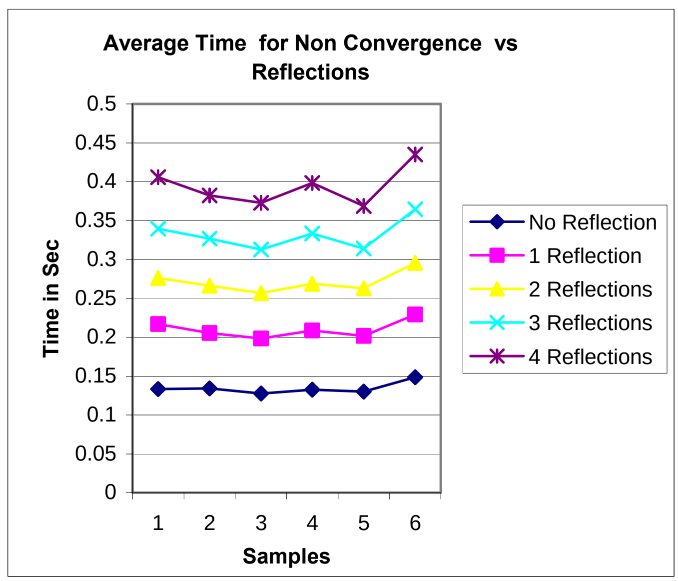

Figure 6. Plot of Non-Convergence time vs samples averaged over 5 Receivers

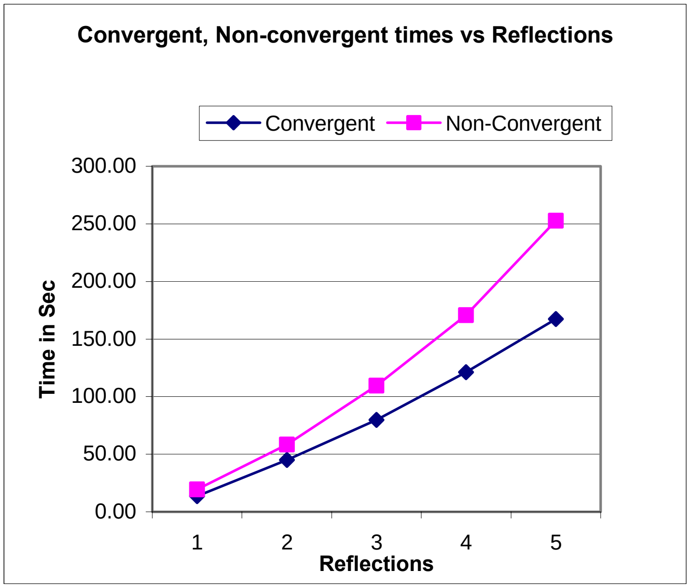

Figure 7. Plot of Convergent and Non-convergent times vs Reflections averaged over 4 TX-RX distances and 5 Receivers

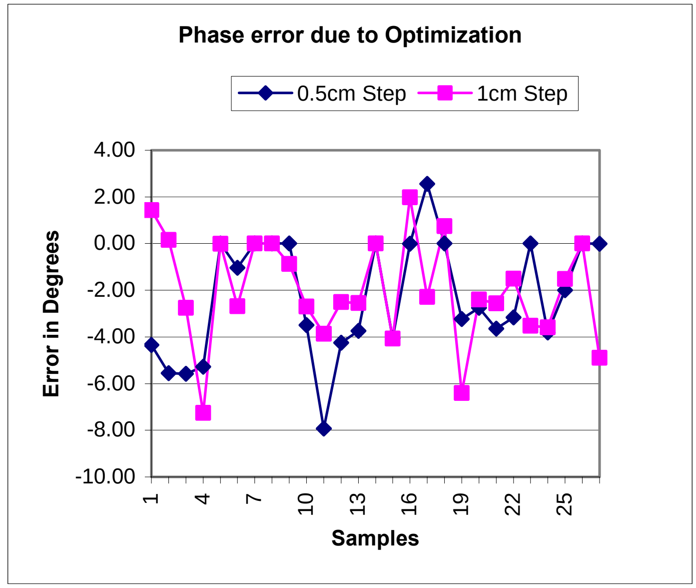

Figure 8. Plot of Phase Error due to optimization algorithm for TX motion along a cube of two different step sizes